





RESEARCH ARTICLE

Testing and assessment of high-precision and high-accuracy AMS-radiocarbon measurements at Nanjing University, China

Hongyan Zhang¹, Huayu Lu¹, Yao Gu¹, Pengyu Lin¹, Jiangfeng Shi¹, Shiyuan Shi¹,
Chenghong Liang¹, Xianyan Wang¹, Wenling An², Tao Ma³ and Steven W Leavitt⁴

¹Laboratory of AMS Dating and the Environment, School of Geography and Ocean Science, Nanjing University, Nanjing, China, ²Institute of Geology and Geophysics, Chinese Academy of Sciences, Beijing, China, ³Department of Archeology and Cultural Relics, Nanjing University, Nanjing, China and ⁴Laboratory of Tree-Ring Research, University of Arizona, Tucson, Arizona, USA
Corresponding author: Hongyan Zhang; Email: hongyan@nju.edu.cn

Received: 28 November 2023; **Revised:** 28 March 2024; **Accepted:** 05 April 2024; **First published online:** 18 September 2024

Keywords: MICADAS; radiocarbon dating; tree-ring ¹⁴C changes; archaeological dating; Late Quaternary chronology

Abstract

In 2018, an Ionplus 200 kV Mini-CARbon DAting System (MICADAS) accelerator mass spectrometer (AMS) was installed at the Laboratory of AMS Dating and the Environment, Nanjing University (NJU-AMS Laboratory), China. The NJU-AMS Laboratory is largely devoted to research on radiocarbon dating and ¹⁴C analysis in fields of earth, environmental and archaeological sciences. The laboratory has successfully employed various pretreatment methods, including routine pretreatment of tree rings, buried wood and subfossil wood, seeds, charcoal, pollen concentrates, organic matter, and shells. In this study, operational status of the NJU-AMS is presented, and results of radiocarbon measurements made on different sample types are reported. Measurements on international standards, references of known age, and blank samples demonstrate that the NJU-AMS runs stably and has good reproducibility on measurement of single samples. The facility is capable of measuring ¹⁴C in samples with the precision and accuracy that meet the requirements for investigating annual ¹⁴C changes, history-prehistory age dating, and Late Quaternary stratigraphic chronology research.

Introduction

Accelerator mass spectrometry (AMS) radiocarbon measurement technology has exceptional sensitivity for ¹⁴C ion detection and smaller sample size requirements compared to the conventional liquid scintillation counting method. Recent development of the compact accelerator mass spectrometer system (Mini CARbon DAting System, MICADAS), which was designed by ETH Zurich and has been commercialized by Ionplus AG Corp, has realized swift and stable high-precision radiocarbon measurement (Wacker et al. 2010a). As a result, this technology has rapidly expanded its application to a wide variety of research areas, including geology (Bronk Ramsey et al. 2008) and archeology (Higham et al. 2014), paleoenvironment reconstruction (Wang et al. 2008), carbon cycle investigation (Burke and Robinson 2021), and even solar activity exploration (Brehm et al. 2021). In this context, a MICADAS was installed at the Laboratory of AMS Dating and the Environment in Nanjing University (NJU-AMS Laboratory) in 2018 (Figure S1). This new laboratory aims to further enhance radiocarbon research capacity of Nanjing University in earth, environmental and archaeological sciences and to provide high-quality ¹⁴C measurements to the scientific community. In this paper we demonstrate the performance and capabilities of the new MICADAS analytical system at Nanjing University by analyzing the precision and accuracy of several different classes of radiocarbon samples. The outcome of which provides effective ¹⁴C accuracy, precision, and dating age limit that can be applied to a wide range of environmental, archaeological, and geochemical studies.

NJU-AMS FACILITIES

The core piece of the NJU-AMS facility is a MICADAS equipped with a 200 kV tandem accelerator employing helium stripping, a cesium sputter ion source capable of accepting both solid and gas cathodes, and a gas ionization detector. Various pretreatment devices are coupled with the MICADAS platform to handle different kinds of samples. A Carbonate Handling System (CHS, IONPLUS™, Switzerland), which employs wet chemistry to handle carbonate samples, and a cube Elemental Analyzer (EA, vario ISOTOPE SELECT, ELEMENTAR™, Germany), used for combustion of organic samples, are both connected to an automated graphitization system (Automated Graphitization Equipment 3 or “AGE3,” IONPLUS™, Switzerland) for solid-sample preparation (ca. 200–1000 µg C). A Gas Interface System (GIS, IONPLUS™, Switzerland) is equipped for small samples (ca. 10–100 µg C). Combustion-derived CO₂ or gas samples can be directly injected into the MICADAS system via the GIS connection. The NJU-AMS Laboratory has achieved a precision of 8‰ (in gaseous standards) in measuring gaseous targets. The GIS has proven to be highly effective in analyzing gaseous and small samples, as demonstrated by numerous applications (e.g. Szidat et al. 2004; Hoffmann et al. 2017; Molnár et al. 2021). Considering that the majority of our current samples are high-precision required and analyzed using solid targets, this study will focus primarily on solid samples. The measurement of gas targets is expected to be further developed and discussed in future research endeavors.

To date, a wide range of sample materials have been analyzed at the NJU-AMS Laboratory, including tree rings, buried wood/subfossil wood, seeds, charcoal, pollen concentrates, loess, peat, lake sediments, and mollusk shells. This paper outlines the radiocarbon measurement protocols of our laboratory and presents the results of selected samples and standards in routine operation, along with the intercomparison results, to showcase the performance of the new NJU-AMS Laboratory.

Chemical Pretreatment and Graphitization

The pretreatment methods utilized on different kinds of samples at the NJU-AMS Laboratory are shown in Figure 1, and the detailed procedures are described in the Supplementary materials (S2).

All chemically pretreated samples are homogenized beforehand. Samples are weighed based on their percent carbon content, and an amount equivalent to 1mg C is preferred. However, if sample size is limited, a minimum of 200 µg C is required to prevent a significant increase in modern carbon contamination throughout the entire preparation and measurement process. The contamination effects are more pronounced when carbon content is less than 200 µg, consequently leading to lower accuracy and precision. A comparative analysis of measurement results on blank samples (Phthalic Anhydride; PhA) with varying carbon contents is provided in the Figure S2 of Supplementary materials (S1). The analysis revealed that background values remained relatively stable within the range of 1000 µg–200 µg C, with an approximate distribution between 50 ka to 47 ka. However, when the sample size drops below 200 µg C, there is a sharp increase in background values as the sample size decreases, highlighting a notable rise in testing uncertainty and contamination, ultimately compromising the reliability of the measurement results. This finding has also been observed by other MICADAS user as well (Haines et al. 2023).

Organic samples are graphitized via EA-AGE3. Samples are flash combusted at a temperature of 920°C in the EA via an on-line combustion system. Under a steady stream of helium carrier gas, oxygen is fed in for 50–120 s (based on sample character) to facilitate a thorough combustion of organic matter and conversion into CO₂. Inorganic samples such as shells or carbonates are graphitized via CHS-AGE3. Acid-cleaned shells are placed in gas-bench 12 mL glass vials, purged with helium, and dissolved in 85% phosphoric acid. The resulting CO₂ obtained from both EA and CHS is then concentrated in a zeolite trap of AGE3 and converted to graphite in the reaction of CO₂ + H₂ → C + H₂O with ca. 5 mg iron catalyst at a temperature of 550°C in separate reaction tubes. Details of graphitization with an AGE3 are described in Wacker et al. (2010b).

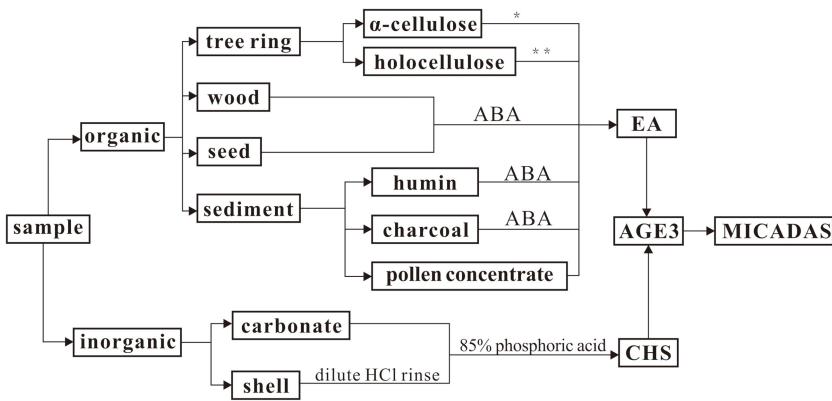


Figure 1. A sketch of procedures for pretreatment utilized on different kinds of samples at the NJU-AMS Laboratory. *The isolation method of α -cellulose follows the procedure of Wieloch et al. (2011). **For some buried woods, we also isolate holocellulose instead of α -cellulose to maximize carbon yield of cellulose and minimize potential contamination introduced by additional processing steps (Němec et al. 2010, Supplementary materials S2). ABA: Acid-Base-Acid pretreatment following standard protocols (e.g. Pessenda et al. 1996; Brock et al. 2010).

To minimize cross-contamination in the graphitization, even though it has been reported to be less than 0.6‰ (Wacker et al. 2010b), samples, standards, and blanks or samples of different matrix are separately prepared in different batches. Moreover, for each batch of standard and blank samples, three additional matrix-matched samples, known as “pre-conditions,” are prepared. Additionally, when dealing with a natural sample of unknown age, an extra matrix-matched pre-condition natural sample is prepared prior to sample graphitization. The “pre-condition” samples undergo EA-combustion/CHS-acidification, similar to regular samples. The resulting CO_2 is collected by the zeolite trap. However, unlike regular samples, the CO_2 generated from pre-condition samples is released before entering the individual reaction tube where graphite is formed.

AMS Measurement

The radiocarbon measurement methods of the MICADAS and its tuning parameters have been described in detail elsewhere (Synal et al. 2007; Suter et al. 2010; Wacker et al. 2010a). Before a routine measurement, the ion source is tuned to an optimal state using standard samples, with a typical current of 30–50 μA for $^{12}\text{C}^-$ ions in the low energy system. After passing through the accelerator with a nearly 48% stable transmission efficiency, the resulting 15–25 μA $^{12}\text{C}^+$ ion beam current is measured in an off-axis Faraday cup in the high energy system, with $^{13}\text{C}/^{12}\text{C}$ ratios of $1.08\text{--}1.09 \times 10^{-2}$.

The standard MICADAS sample holder (magazine) contains 39 positions for each batch loading. Typically, a batch comprises seven oxalic acids (OXII, NIST SRM 4990c), six or seven chemical blanks (PhA or PhA & IAEA-C1), one IAEA-C7 and one IAEA-C8 references, one or two samples of known age and blank samples with the same matrix as the natural samples (normally used as reference) and 20~22 samples of un-known age. During automatic measurements, the Accelerator Control Software (ACS, IONPLUS™, Switzerland) measures the whole magazine over several passes with 5 minutes spent passing through each position. The total measurement time for a single sample depends on both the anticipated measurement precision and the ^{14}C content in the sample matrix. For samples with high-precision requirements, an increase in measurement time will be carried out to reduce statistical uncertainty. For example, when dating Late Pleistocene Chinese loess, which has a relatively low ^{14}C fraction, a minimum of 10 passes (usually ca. 15 passes, equivalent to 4500 seconds of measuring time) are necessary, while for the ancient wood samples, 8 passes (equivalent to 2400 seconds of measuring

Table 1. The measured $F^{14}C$ and $\delta^{13}C$ mean values obtained from background samples, standards and reference samples at NJU-AMS Laboratory during its first three years of routine operation, compared to the corresponding reported values (Mann 1983; Le Clercq et al. 1997; Stuiver 1983). All the PhA and IAEA-C1 values are reported without blank subtraction. The OXII, IAEA-C7, and C8 values have been blank-corrected using the mean results of PhA within the measuring batch for organic samples or by the mean values of all the PhA and IAEA-C1 within the measuring batch for carbonates. The measured $F^{14}C$ mean values are presented as arithmetic mean \pm standard error of the mean. SD represents the standard deviation of the individual sample results

Samples	Measured $F^{14}C$ mean value	SD	Reference $F^{14}C$ value	Measured mean value of $\delta^{13}C$ (‰) VPDB	Reference $\delta^{13}C$ (‰) VPDB	N analyses
PhA	0.00242 ± 0.00004	0.0008	—	−30	—	439
IAEA-C1	0.00224 ± 0.00011	0.0008	—	2.1	2.4	50
OXII	1.34069 ± 0.00010	0.0024	1.34066 ± 0.00043	−17.8	−17.8	539
IAEA-C7	0.4947 ± 0.00019	0.0017	0.4953 ± 0.0012	−14.5	−14.5	80
IAEA-C8	0.1504 ± 0.00010	0.0010	0.1503 ± 0.0017	−18.3	−18.7	85

time) are optimal and can produce high precision (<2‰) results (as demonstrated in Aerts-Bijma et al. 2021). The data reduction program “BATS” (IONPLUS™, Switzerland; Wacker et al. 2010c) included in MICADAS is used to automatically calculate standard-and blank-corrected results for measured samples. In BATS, standards, blanks, and samples of un-known age are each assigned unique identifier codes, enabling direct access to standard and blank information stored in the database. Typically, in our case, within a batch of measured samples, the weighted mean of all individual OXII measured results is utilized for data normalization. When analyzing organic samples, the weighted mean of all individual PhA measured results is used for blank-correction, while for carbonate samples, the weighted mean of all individual PhA and C1 measured results is subtracted. References such as IAEA-C7 and C8, along with matrix-matched blanks and samples of known age, are commonly employed for quality control purposes. Moreover, BATS allows us to introduce and utilize other standards (e.g. IAEA-C7, IAEA-C8) or blanks (e.g. matrix-matched blanks) that measured simultaneously with the samples for normalization or blank-correction when deemed necessary. All corrections are applied to the results of individual measurements for all samples before calculating any related means. Conventional radiocarbon ages can be converted to calendar ages using the latest version of the calibration curve published by OxCal online (URL: <https://c14.arch.ox.ac.uk>) if needed.

Results and Discussion

Blanks and Standards

In order to evaluate performance in the routine analyses at NJU-AMS, Fraction Modern ($F^{14}C$) results for all blanks and standards processed in the first 3 years by NJU-AMS are given in Table 1. For blanks, the mean measured $F^{14}C$ value for PhA is 0.00242 ± 0.00004 (arithmetic mean of measured results on individual samples \pm standard error, $n = 439$), equivalent to a radiocarbon age of ca. 49 ka BP. The average $F^{14}C$ for IAEA-C1 is 0.00224 ± 0.00011 (arithmetic mean of measured results on individual samples \pm standard error, $n = 50$), equivalent to a radiocarbon age of ca. 50 ka BP. These results reflect the average background level observed across a wide variety of natural sample measurements processed by the NJU-AMS. However, it is important to note that certain samples required expedited processing and were not measured at highest precision. Consequently, they underwent shorter measurement times, leading to slightly elevated $F^{14}C$ values in the corresponding blanks. It is worth mentioning that longer measurement durations help mitigate the impact of surface contamination on the final $F^{14}C$ results of all

samples. So far, we have not observed the onset of enhancement in background levels when testing samples from the “Bomb-peak” period, indicating the absence of apparent cross-contamination between natural samples throughout the AMS measurement process.

The NIST OXII (SRM 4990C) is used as a primary standard to normalize measurements for the MICADAS transmission and fractionation. The 539 analyses of OXII with independent graphitization in routine operation of NJU-AMS during the first three years provided an average $F^{14}\text{C}$ of 1.34069 ± 0.00010 (arithmetic mean of measured results on individual samples \pm standard error), which is in good agreement with the consensus value of 1.34066 ± 0.00043 (Mann 1983; Stuiver 1983) (Table 1 and Figure 2a). The standard deviation of the individual measurements ($0.0024 F^{14}\text{C}$) is comparable with the uncertainty from the counting statistics and the blank correction of $0.0023 F^{14}\text{C}$. Therefore, precision for routine OXII standards measurements is ca. 1.8%. As a reference sample, the measured mean $F^{14}\text{C}$ value for the IAEA-C7 of 0.4947 ± 0.00019 (arithmetic mean of measured results on individual samples \pm standard error, $n = 80$) is within the error range of the reported $F^{14}\text{C}$ value of 0.4953 ± 0.0012 (Le Clercq et al. 1997) (Table 1 and Figure 2b). The standard deviation of the individual results ($0.0017 F^{14}\text{C}$) is 0.6% higher than the uncertainty from counting statistics and the blank correction for a single measurement ($0.0011 F^{14}\text{C}$). Also, the IAEA-C8 $F^{14}\text{C}$ mean value of 0.1504 ± 0.00010 (arithmetic mean of measured results on individual samples \pm standard error, $n = 85$) is in perfect agreement with the reported $F^{14}\text{C}$ mean value of 0.1503 ± 0.0017 (Le Clercq et al. 1997) (Table 1 and Figure 2c). The standard deviation of the individual measurements ($0.0010 F^{14}\text{C}$) is comparable with the uncertainty from the counting statistics and the blank correction of $0.0007 F^{14}\text{C}$. Because these references are processed at the beginning of sample graphitization, we therefore conclude that the uncertainty introduced by sample preparation and graphitization is not significant. Nevertheless, typically, a relative 1% external error was added to the final reported uncertainties for all the individual references and samples to account for reproducibility of sampling and preparation. This value was estimated from the long-term replicate analysis of the reference material and intercomparisons. For a more detailed calculation process about the added external error, please refer to the original literature (Wacker et al. 2010c, Eq. 16, 17 and 18).

In Figure 2, there is a noticeable increase in the dispersion of the standard and reference measurement results over time. The main factor contributing to this heightened dispersion after a trial period of operation is the diverse precision requirements for different samples. As the testing scope expands following the trial period, various samples require different levels of testing precision, leading to fluctuations in standards and references. Additionally, as the number of samples grows, high-precision samples are typically measured promptly after preparation, while samples with lower precision requirements may wait in queue for over two weeks, increasing the risk of surface contamination. Overall, the precision obtained through long-term measurements on OXII standards is approximately 1.8%, which would be even better for purely high-precision measurements.

Annual Tree-Ring ^{14}C Changes

Tree rings can offer independently dated exact measures of past atmospheric radiocarbon levels, which are controlled by solar activity or modern human activity like H-bomb testing (e.g. Stuiver et al. 1998; Reimer et al. 2020). High-precision and high-accuracy ^{14}C dating results in finely resolved probability distributions of calibrated ages. However, natural fluctuations in atmospheric ^{14}C levels at sub-centennial timescales are quite delicate (Damon et al. 1973; Stuiver and Braziunas 1993). The current annual decrease in atmospheric $F^{14}\text{C}$ is relatively several thousandths (Levin et al. 2013), posing a challenge for ^{14}C dating of modern samples using bomb period ^{14}C . The post-bomb era tropospheric $^{14}\text{CO}_2$ content has been multiply measured directly in zonal atmospheric samples (Hua et al. 2021). This provided an opportunity to test the precision and accuracy of our tree-ring ^{14}C measurement results. We measured a series of dendrochronologically dated tree-ring samples for the period AD 2004 to 2014 which were collected from the southern Himalayas (An et al. 2019). They should reflect the tropospheric

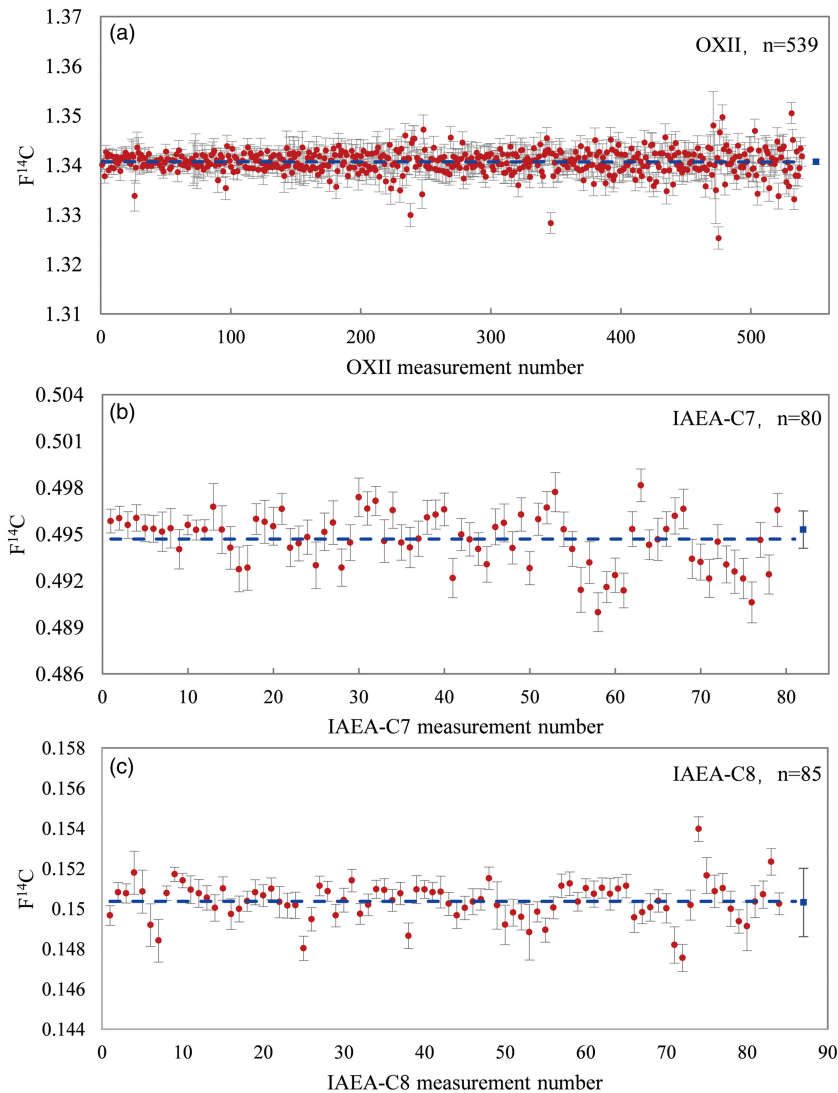


Figure 2. The measurement results of standard OXII (a), and reference materials IAEA-C7 (b), and IAEA-C8 (c) over the first three years of operation at the NJU-AMS Laboratory. All the individual OXII, IAEA-C7, and C8 values have been blank-corrected using weighted mean of all the PhA results in the same batch if the concurrently measured real samples are organic matter or by weighted mean of all the PhA and IAEA-C1 results in the same batch if the concurrently measured real samples are carbonates. The analysis runs are arranged chronologically from earliest on the left to most recent on the right. The red points, along with their error bars ($1-\sigma$), represent the individual $F^{14}C$ values obtained at the NJU-AMS Laboratory, while the blue-dashed lines indicate their corresponding arithmetic mean values. The blue squares at the right side of each panel display the corresponding reference values along with their reported errors as provided in the literature (Mann 1983; Stuiver 1983; Le Clercq et al. 1997).

$^{14}CO_2$ levels in zone 2 of the Northern Hemisphere. We compared our measurement results with the related observed tropospheric $^{14}CO_2$ data, as shown in Figure 3. The entire process of cellulose extraction, graphitization, and AMS measurement of the samples was completed at the NJU-AMS Laboratory. The 11 single-year tree-ring cellulose samples were measured to a precision

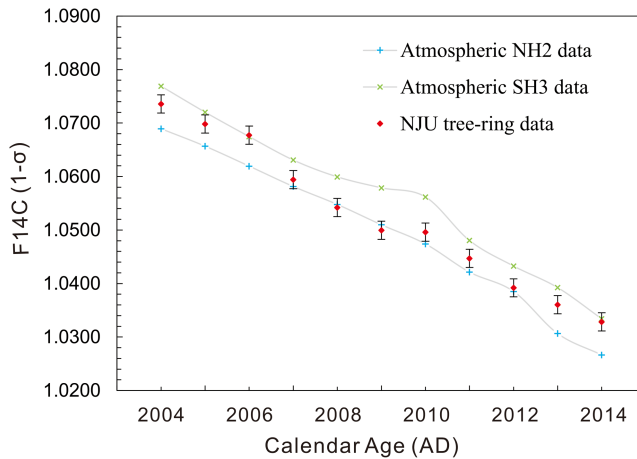


Figure 3. The annual tree-ring samples from the Himalayas measured at the NJU-AMS Laboratory are plotted with $1-\sigma$ uncertainties together with 12-month average of atmospheric $F^{14}C$ record for each Zone 2 of the Northern Hemisphere (NH2) and Zone 3 of the Southern Hemisphere (SH3) (Hua et al. 2021). The data for NH2 and SH3 are represented by a dotted line, while the tree-ring data from NJU-AMS Laboratory are shown using a scatter plot.

of ca. $0.0017 F^{14}C$ (1σ , 1.6‰), including an estimated external uncertainty for the sample preparation of 1‰.

The atmospheric $F^{14}C$ records of Northern Hemisphere Zone 2 (NH2) and Southern Hemisphere Zone 3 (SH3) are the average of compiled monthly data in Zone 2 of the Northern Hemisphere and Zone 3 of Southern Hemisphere for each year, respectively (Hua et al. 2021). Plots in Figure 3 show the three sets of data. From Figure 3, it can be observed that the tree-ring ^{14}C data of the study area fall within a similar range as the atmospheric ^{14}C data from zones NH2 and SH3 (in range between 1.0260 and 1.0770 $F^{14}C$) and exhibit a decreasing rate of approximately $0.004 F^{14}C$ year by year. However, the tree-ring ^{14}C data from the study area, which should locate in zone NH2, are significantly above the atmospheric ^{14}C data of NH2. The average deviation of tree-ring ^{14}C from the NH2 data is $0.0032 F^{14}C$, with a maximum deviation reaching $0.0066 F^{14}C$, which cannot be explained by the measurement errors or the seasonal variations in atmospheric ^{14}C . Surprisingly, the tree-ring ^{14}C data consistently fall between the atmospheric NH2 and SH3 data, approaching NH2 in some years and closer to SH3 in others. These results have prompted us to consider whether the atmospheric ^{14}C levels revealed in our data might reflect or contain the elevated atmospheric ^{14}C information of the Southern Hemisphere in the study years. Previous studies on oxygen isotopes in tree rings from the same site suggest that the source of moisture during the tree-ring growth season is attributed to the Indian summer monsoon (An et al. 2019). Therefore, we assumed that throughout the growing season, as the Intertropical Convergence Zone (ITCZ) shifts northward to the Northern Hemisphere, the southeast trade winds from the Southern Hemisphere cross the equator and change direction to establish the Indian summer monsoon, facilitating the transportation of atmospheric ^{14}C information from the Southern Hemisphere. Tree-ring ^{14}C investigations from the Little Ice Age and the pre-bomb period in north-central Thailand (Hua et al. 2004a, 2004b), where further south than our study area, also confirm the impact of Southern Hemisphere air parcels on the Northern Hemisphere tree-rings. Conducting long-term, high-precision tree-ring ^{14}C studies in the Himalayas will further enhance our comprehension of atmospheric exchange patterns across hemispheres. This study demonstrated that the precision and accuracy of the NJU-AMS Laboratory is sufficient for investigating subtle ^{14}C variations within tree rings.

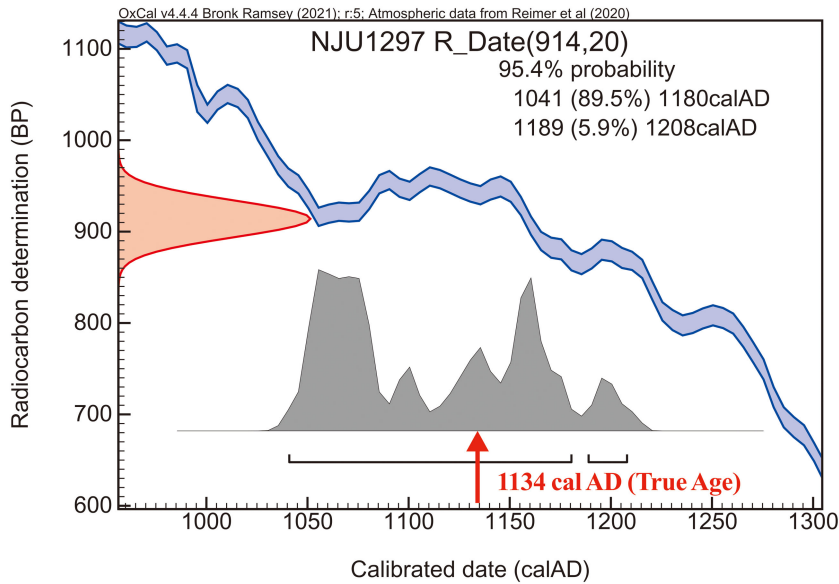


Figure 4. Calibration of charred plant residuals from the Song Dynasty kiln site. Radiocarbon age calibration using IntCal20 (Reimer et al. 2020) and OxCal version 4.4 (Bronk Ramsey 2021).

History-Prehistory Age Dating

Dating materials from archaeological sites during historical periods, which have real calendar-year context, provides opportunities to examine the accuracy of our radiocarbon dating results. We analyzed a charred plant residue present in the production clay of a kiln site located in the lower reaches of the Yangtze River in China, dating to the Song Dynasty. Following the processing protocols described above, we obtained a radiocarbon age of 914 ± 20 BP (1σ , including 1‰ uncertainty for sampling). We calibrated this age using IntCal20 (Reimer et al. 2020), but because of the plateau of the calibration curve during the 11th to 13th centuries AD, we obtained an age range of cal AD 1041–1208 (95.4% probability) (Figure 4). Even so, the calibrated age range with the greatest probability (89.5%) spans cal AD 1041–1180, is consistent with the true age of AD 1134 incised as part of the inscription on the bricks.

To further test accuracy, we joined the inter-comparison dating campaign that also includes the AMS laboratories of University of Tokyo, Peking University, and Beta Analytic Testing Laboratory, processing a prehistoric cultural site. It is an early Hemudu cultural site that was temporarily used as a harbor for fishing and hunting, and then abandoned due to the rising sea level (Zhejiang Provincial Institute of Cultural Relics and Archaeology et al. 2021). The selected 8 samples including 2 organic residues, 4 wood or twigs, and 2 peach pits were all pretreated and measured at the NJU-AMS Laboratory. The compiled radiocarbon dating results were reported in the range of 7800–8300 cal BP <URL: <https://baijiahao.baidu.com/s?id=1668364373751341440&wfr=spider&for=pc>>, and part of the results from Peking University has also been published elsewhere recently (Zhejiang Provincial Institute of Cultural Relics and Archaeology et al. 2021). All the samples were measured to a precision <math><2\text{‰}</math> (including 1‰ external uncertainty). The ^{14}C age values were calibrated by IntCal20. The intercomparison (Figure 5) shows that the NJU-AMS Laboratory results are in excellent agreement with those of the other 3 laboratories, validating the sample processing methods for a range of material types at the NJU-AMS Laboratory.

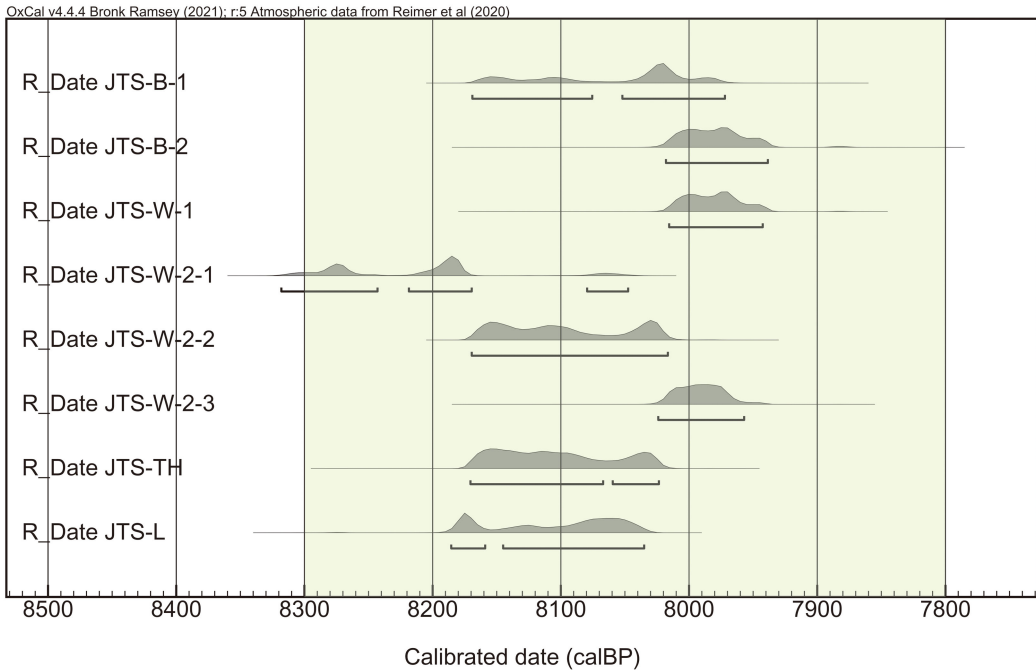


Figure 5. Calibrated ^{14}C ages of 8 samples determined by the NJU-AMS Laboratory. The green shaded area represents value range of calibrated ^{14}C age obtained by other three institutions including University of Tokyo, Peking University, and Beta Analytic (Zhejiang Provincial Institute of Cultural Relics and Archaeology et al. 2021).

Late Quaternary Stratigraphic Dating

High-precision radiocarbon dating of the Late Pleistocene deposits (<50 ka) is a challenge due to, as other researchers have mentioned, carbon reservoir effects (Zhou et al. 2022), and the mixture of carbon sources at different ages or contamination with modern carbon in the dating material (Brown 1997; Colman et al. 1996; Long et al. 2015). Here, we provide a group of five Late Quaternary interstadial ^{14}C dating results (Table 2) processed by the NJU-AMS Laboratory in cooperation with the Laboratory of Tree-Ring Research at the University of Arizona. The five samples all represent the outer 12 to 30 tree rings of subfossil log samples collected from the interstadial beds of the Great Lakes basin. Sample #1 was collected from surface muck soil materials in the modern wetland at the Tower site in northern Michigan, USA (Schaezel et al. 2013). Samples from this site had previously been dated at ca. 2500 to 10,100 ^{14}C yr BP. The other four samples were all collected from Two Creeks-age deposits in east-central Wisconsin, USA, one (#2) of which came from the classic Two Creeks type locality of the Late Pleistocene glacial/interstadial transition. The Two Creeks wood is typically found within red clayey deposits of glacial till and fine lake sediments. More than one hundred Two Creeks wood samples have been collected and dated over the last 50 years and fall into the range of 12,400 and 11,200 ^{14}C yr BP (Broecker and Farrand 1963; Kaiser 1994; Leavitt et al. 2007; Panyushkina and Leavitt 2007), which represents the date of the last major glacial advance in the continental USA. Two subsamples of sample #5 had been pretreated with the ABA method and then dated at the Accelerator Mass Spectrometer Laboratory, University of Arizona in 2009, giving uncalibrated ages of $11,887 \pm 61$ BP for the outer 10 rings and $11,739 \pm 63$ BP for the inner 10 rings.

As the samples we received were somewhat fragmented, each sample was randomly sampled after crushing and homogenization, and the possible uncertainties introduced will be considered in the final dendrochronologically calibrated radiocarbon dating results. Processing with our protocols described

Table 2. List of the single measurement of fossil woods from Late Quaternary interstadials with their mean values, given in ^{14}C yr BP with $\pm 1\sigma$ uncertainties

Sample no.	Lab code	Sample name	Strata	F ^{14}C	Error	^{14}C yr BP	\pm year
A#1	NJU1633.1.1	UA-TSSL-8a	Surface muck	0.5769	0.0011	4419	15
	NJU1633.1.2			0.5770	0.0012	4417	17
Mean of samples (n = 2)						4418	11
A#2	NJU1634.1.1	UA-TCWM-100	Two Creeks	0.2319	0.0006	11739	22
A#3	NJU1635.1.1	UA-EQJL-100(A)		0.2319	0.0006	11739	22
A#4	NJU1636.1.1	UA-EQJL-101(B)		0.2322	0.0006	11730	21
A#5	NJU1291.1.1	UA-TRAS-2		0.2321	0.0006	11732	21
Mean of samples (n = 4)						11735	11

above, the reproducibility of high-precision measurements on the five wood samples is given in Table 2. The five samples from the Tower site and the Two Creeks-age deposits show two distinct ages with perfect repeatability within their final uncertainties of ca. 16 and 22 ^{14}C yr (ca. 2‰, including 1‰ estimated uncertainty in sampling and pretreatment). The dating results of the four sub-samples (sample #2–5) from Two Creeks closely match the uncalibrated ages of #5 sample provided by Arizona University and the previously published Two Creeks wood dating results, confirming the higher accuracy of NJU-AMS Laboratory in measuring Late Quaternary stratigraphic samples. The remarkable consistency between the two repeated measurements at the Tower site and the low standard deviation of approximately 0.6‰ in the results of the four sub-samples from Two Creeks wood indicate that the capability of NJU-AMS for high-precision measurement may exceed our estimation (as provided in Table 2, 1σ errors are about 2‰ for individual measurements). This suggests that for high-precision measurements, the external errors we added to the natural samples may have been overestimated. This study provides confidence that when the dating material is representative and well preserved, robust, high-precision radiocarbon dating by a single measurement (finite ages approaching 50,000 years) can be obtained on Late Quaternary deposits. A key point is to fully understand the relevant sedimentary and burial environment and to ensure close communication between the laboratory work and the field work.

Conclusions

Following the processing protocols of the NJU-AMS Laboratory, we have demonstrated reliable radiocarbon analysis of wood, tree rings, organic residue, and plant tissues from the broad suit of materials (cellulose of tree rings, wood, charcoal, organic remains, pollen concentrates, and shells of Mollusks) that our lab specializes in. Results for international standards in the first three years of operation confirm that the NJU-AMS runs stably and has good reproducibility on single measurements. The results from blanks provide confidence that the NJU-AMS Laboratory is well-equipped to measure ^{14}C samples from the present to ca. 50,000 years ago (through multiple measurements for ages near this limit). Precision and accuracy of radiocarbon measurements at the NJU-AMS Laboratory can satisfy requirements for investigating zonal and annually changing ^{14}C activities, conducting age dating of historical and prehistorical artifacts, and establishing Late Quaternary stratigraphic chronology.

Supplementary material. To view supplementary material for this article (Figure S1 and S2 is given in Supplementary materials S1, and details of pretreatment processes for different sample materials are provided in Supplementary materials S2), please visit <https://doi.org/10.1017/RDC.2024.70>.

Acknowledgments. We express our gratitude to Professor Jianqiu Huang and Guoping Sun for their assistance in sample collection, and to Dr. Yesi Zhao and Kehan Shao for their support in sample pretreatment. Additionally, we appreciate the valuable input from the two anonymous reviewers. This research is supported by the Project of the National Natural Science Foundation of China (42171155) and A Project Funded by the Priority Academic Program Development of Jiangsu Higher Education Institutions (PAPD).

References

- Aerts-Bijma A, Paul D, Dee M, Palstra S and Meijer H (2021) An independent assessment of uncertainty for radiocarbon analysis with the new generation high-yield accelerator mass spectrometers. *Radiocarbon* **63**, 1–22.
- An W, Xu C, Liu X, Tan N, Sano M, Li M, Shao X, Nakatsuka T and Guo Z (2019) Specific response of earlywood and latewood $\delta^{18}\text{O}$ from the east and west of Mt. Qomolangma to the Indian summer monsoon. *Science of the Total Environment* **689**, 99–108.
- Brehm N, Bayliss A, Christl M, Synal HA, Adolphi F, Beer J, Kromer B, Muscheler R, Solanki SK, Usoskin I, et al. (2021) Eleven-year solar cycles over the last millennium revealed by radiocarbon in tree rings. *Nature Geoscience* **14**(1):10–15.
- Brock F, Higham T, Ditchfield P and Bronk Ramsey C (2010) Current pretreatment methods for AMS radiocarbon dating at the Oxford Radiocarbon Accelerator Unit (ORAU). *Radiocarbon* **52**, 103–112.
- Broecker W and Farrand W. 1963. Radiocarbon age of the Two Creeks Forest bed, Wisconsin. *Geological Society of America Bulletin* **74**, 795–802.
- Bronk Ramsey C (2008) Deposition models for chronological records. *Quaternary Science Reviews* **27**, 42–60.
- Bronk Ramsey C (2021) OxCal 4.4.4 URL: <<https://c14.arch.ox.ac.uk/oxcal/OxCal.html#>>
- Brown A (1997) *Alluvial Geoarchaeology: Floodplain Archaeology and Environmental Change*. Cambridge (UK): Cambridge University Press, 63–103.
- Burke A and Robinson L (2021) The Southern Ocean's role in carbon exchange during the last deglaciation. *Science* **335**, 557–561.
- Colman S, Jones G, Meyer R, King J, Peck J and Orem S (1996) AMS radiocarbon analyses from Lake Baikal, Siberia: challenges of dating sediments from a large, oligotrophic lake. *Quaternary Science Reviews* **15**, 669–684.
- Damon PE, Long A and Wallick EI (1973) Magnitude of 11-year radiocarbon cycle. *Earth and Planetary Science Letters* **20**, 300–306.
- Haines AH, Hiscock TW, Palmer JG, Turney CSM, Thomas ZA, Cadd H, Vohra J and Marjo CE (2023) The accuracy and precision of small-sized modern wood samples analyzed at the Chronos 14carbon-Cycle Facility. *Radiocarbon* 1–11.
- Hoffmann H, Friedrich R, Kromer B and Fahrni S (2017) Status report: Implementation of gas measurements at the MAMS ^{14}C AMS facility in Mannheim, Germany. *Nuclear Instruments and Methods in Physics Research, Section B: Beam Interactions with Materials and Atoms* **410**, 184–187.
- Hua Q, Barbetti M and Zoppi U (2004a) Radiocarbon in annual tree rings from Thailand during the pre-bomb period, AD 1938–1954. *Radiocarbon* **46**(2), 925–932.
- Hua Q, Barbetti M, Zoppi U, Fink D, Watanasak M and Jacobsen GE (2004b) Radiocarbon in tropical tree rings during the Little Ice Age. *Nuclear Instruments and Methods in Physics Research B* **223–224**, 489–494.
- Hua Q, Turnbull J, Santos G, Rakowski A, Ancapichun S, De Pol-Holz R, Hammer S, Levin I, Miller J, et al. (2021) Atmospheric radiocarbon for the period 1950–2019. *Radiocarbon* **64**(4), 723–745.
- Higham T, Douka K, Wood R, Bronk Ramsey C, Brock F, Basell L, Camps M, Arrizabalaga A, Baena J, Barroso-Ruiz C, et al. (2014) The timing and spatiotemporal patterning of Neanderthal disappearance. *Nature* **512**, 306–309.
- Kaiser K (1994) Two Creeks interstade dated through dendrochronology and AMS. *Quaternary Research* **42**, 288–298.
- Leavitt S, Panyushkina I, Lange T, Cheng L, Schneider A and Hughes J (2007) Radiocarbon “wiggles” in great lakes wood at about 10,000 to 12,000 BP. *Radiocarbon* **49**, 855–864.
- Le Clercq M, van der Plicht J and Gröning M (1997) New ^{14}C reference materials with activities of 15 and 50 PMC. *Radiocarbon* **40**, 295–297.
- Levin I, Kromer B and Hammer S (2013) Atmospheric $\Delta^{14}\text{CO}_2$ trend in Western European background air from 2000 to 2012. *Tellus B* **65**, 20092.
- Long T and Taylor D (2015) A revised chronology for the archaeology of the lower Yangtze, China, based on Bayesian statistical modelling. *Journal of Archaeological Science* **63**, 115–121.
- Mann W (1983) An international reference material for radiocarbon dating. *Radiocarbon* **25**, 519–527.
- Molnár M, Mészáros M, Janovics R, Major I, Hubay K, Buró B, Varga T, Kertész T, Gergely V, Vas Á, Orsovski G, Molnár A, Veres M, Seiler M, Wacker L and Jull AJT (2021) Gas ion source performance of the EnvironMICADAS at HEKAL Laboratory, Debrecen, Hungary. *Radiocarbon* **63**(2), 499–511.
- Němec M, Wacker L, Hajdas I and Gäggeler H (2010) Alternative methods for cellulose preparation for AMS measurement. *Radiocarbon* **52**(2–3), 1358–1370.
- Panyushkina I and Leavitt S (2007) Insights into Late Pleistocene-early Holocene Paleoeology from fossil wood around the Great Lakes region. In Hooyer TS (ed), *Late-Glacial History of East Central Wisconsin: Wisconsin Geological and Natural History Survey Open-File Report*, 47–57.
- Pessenda L, Valencia E, Camargo P, Telles E, Martinelli L, Cerri C, Aravena R and Rozanski K (1996) Natural radiocarbon measurements in Brazilian soils developed on basic rocks. *Radiocarbon* **38**, 203–208
- Reimer PJ, Austin WEN, Bard E, Bayliss A, Blackwell PG, Bronk Ramsey C, Butzin M, Cheng H, Edwards RL, Friedrich M et al. (2020) The IntCal20 Northern Hemisphere radiocarbon age calibration curve (0–55 cal kBP). *Radiocarbon* **62**, 725–757.
- Schäetzl RJ, Yansa CH and Leuhmann MD (2013) Paleobotanical and environmental implications of a buried forest bed in northern Lower Michigan, USA. *Canadian Journal of Earth Sciences* **50**, 483–493.
- Stuiver M (1983) International agreements and the use of the new oxalic-acid standard. *Radiocarbon* **25**, 793–795.

- Stuiver M and Braziunas TF (1993) Sun, ocean, climate and atmospheric ^{14}C : an evaluation of causal and spectral relationships. *Holocene* **3**, 289–305.
- Stuiver M, Reimer PJ, Bard E, Beck JW, Burr GS, Hughen KA, Kromer B, McCormac G, van der Plicht J and Spurk M (1998) IntCal98 radiocarbon age calibration, 24,000–0 cal BP. *Radiocarbon* **40**, 1041–1083.
- Synal HA, Stocker M and Suter M (2007) MICADAS: a new compact radiocarbon AMS system. *Nuclear Instruments and Methods in Physics Research Section B: Beam Interactions with Materials and Atoms* **259**, 7–13.
- Suter M, Müller A, Alifimov V, Christl M, Schulze-König T, Kubik P, Synal HA, Vockenhuber C and Wacker L (2010) Are compact AMS facilities a competitive alternative to larger tandem accelerators? *Radiocarbon* **52**, 319–330.
- Szidat S, Jenk TM, Gäggeler HW, Synal HA, Hajdas I, Bonani G and Saurer M (2004) THEODORE, a two-step heating system for the EC/OC determination of radiocarbon (^{14}C) in the environment. *Nuclear Instruments and Methods in Physics Research B* **223–224**, 829–836.
- Wacker L, Bonani G, Friedrich M, Hajdas I, Kromer B, Němec M, Ruff M, Suter M, Synal HA and Vockenhuber C (2010a) MICADAS: routine and high-precision radiocarbon dating. *Radiocarbon* **52**(2), 252–262.
- Wacker L, Němec M and Bourquin J (2010b) A revolutionary graphitisation system: fully automated, compact and simple. *Nuclear Instruments and Methods in Physics Research B* **268**, 931–934.
- Wacker L, Christl M and Synal HA (2010c) Bats: a new tool for AMS data reduction. *Nuclear Instruments and Methods in Physics Research B* **268**, 976–979.
- Wang YJ, Cheng H, Edwards R, Kong X, Shao X, Chen S, Wu J, Jiang X, Wang X and An Z (2008) Millennial- and orbital-scale changes in the East Asian monsoon over the past 224,000 years. *Nature* **451**, 1090–1093.
- Wieloch T, Helle G, Heinrich I, Voigt M and Schyma P (2011) A novel device for batch-wise isolation of α -cellulose from small-amount wholewood samples. *Dendrochronologia* **29**, 115–117.
- Zhejiang Provincial Institute of Cultural Relics and Archaeology, Ningbo Institute of Cultural Heritage Management, Yuyao Hemudu Site Museum (2021) Zhejiang Yuyao Jingtoushan Neolithic site [in Chinese]. *Archaeology* **7**, 3–26.
- Zhou W, Chui Y, Yang L, Cheng C, Chen N, Ming G, Hu Y, Li W and Lu X (2022) ^{14}C Geochronology and radiocarbon reservoir effect of reviewed lakes study in China. *Radiocarbon* **64**(4), 833–844.

Cite this article: Zhang H, Lu H, Gu Y, Lin P, Shi J, Shi S, Liang C, Wang X, An W, Ma T, and Leavitt SW (2024). Testing and assessment of high-precision and high-accuracy AMS-radiocarbon measurements at Nanjing University, China. *Radiocarbon* **66**, 568–579. <https://doi.org/10.1017/RDC.2024.70>